Neuron J is a Rapid and Reliable Open Source Tool for Evaluating Corneal Nerve Density in Herpes Simplex Keratitis

Paul Cottrell,[1,2] Sohail Ahmed,[1] Catherine James,[1] James Hodson,[3] Peter J. McDonnell,[1] Saaeha Rauz,[1] and Geraint P. Williams[1]

[1]Academic Unit of Ophthalmology, Birmingham and Midland Eye Centre, School of Immunity and Infection, College of Medical and Dental Science, University of Birmingham, Birmingham, United Kingdom
[2]Department of Optometry, Birmingham and Midland Eye Centre, City Hospital, Birmingham, United Kingdom
[3]Department of Statistics, Wolfson Computer Laboratory, University Hospitals Birmingham NHS Foundation Trust, Birmingham, United Kingdom

Correspondence: Geraint P. Williams, Academic Unit of Ophthalmology, School of Immunity and Infection, College of Medical and Dental Sciences, Birmingham and Midland Eye Centre, City Hospital, Birmingham B15 2WB, UK; g.p.williams@bham.ac.uk.

SR and GPW are joint senior authors.

Submitted: July 1, 2014
Accepted: October 5, 2014

Citation: Cottrell P, Ahmed S, James C, et al. Neuron J is a rapid and reliable open source tool for evaluating corneal nerve density in herpes simplex keratitis. *Invest Ophthalmol Vis Sci*. 2014;55:7312–7320. DOI:10.1167/iovs.14-15140

Purpose. In vivo confocal microscopy (IVCM) demonstrates reduction in corneal sub-basal nerve density in herpes simplex keratitis (HSK). Image J is an open source image-analysis platform that can be combined with a nerve tracer, Neuron J. We sought to compare the reliability and speed of corneal nerve density quantification between these modalities and their relation to clinical damage.

Methods. A total of 16 eyes (14 patients) with chronic HSK was assessed clinically and by IVCM. Randomly ordered triplicate, representative images from the central cornea were presented to two masked observers and corneal sub-basal nerve density was measured using Image J/Neuron J. Agreement was quantified using intraclass correlation coefficients (ICC), Bland-Altman plots together with mean difference, and level of agreement (LoA).

Results. The median nerve density was measured at 7.1 mm/mm^2 (quartiles, 3.3–11.2), with Neuron-J demonstrating good intra-/interobserver agreement (ICC, 0.96–0.99; $P < 0.001$; mean difference, 0.1–1.4; LoA, $<\pm 3.3$). Intraeye reliability was less consistent (mean difference, 1.7–2.3; LoA, ±8.8–9.8). Neuron J was highly comparable to Image J for both observers (ICC, 1.0; $P < 0.001$; mean difference, <0.2; LoA, $\pm<1.2$) and significantly faster than Image J (median, 49 vs. 102 seconds, $P < 0.001$). Diminished nerve density was associated with corneal opacification and reduction in visual acuity (both $P = 0.03$).

Conclusions. The IVCM combined with Neuron J affords objective, user-friendly, and fast quantification of corneal nerve damage in HSK. It provides semiobjective phenotyping of the sequelae of neurotrophic corneal damage and offers a potential tool for measuring vulnerability to relapse or additional infections. Further exploration in a larger longitudinal cohort is warranted.

Keywords: Herpes simplex, Neuron J, Image J, corneal nerve density

Herpes simplex virus (HSV) 1 and 2 are alpha-herpes viruses transmitted through close human contact resulting in conditions, such as cutaneous herpes or herpes simplex labialis. Viral reactivation results in anterograde transport from the root ganglion to distal nerve endings, such as the trigeminal ganglion to the cornea.[1] At this site, HSV (primarily HSV 1) is responsible for localized corneal inflammation known as herpes simplex keratitis (HSK), resulting in vision loss complications due to vascularization, scarring, ocular surface failure, and secondary bacterial infections.

Recurrent HSK also can lead to loss of corneal sensitivity by destruction of the corneal nerve plexus. The corneal nerve plexus is composed of terminal nerve endings emanating from branches of the ophthalmic division of the trigeminal nerve. Nerves enter peripherally, losing their myelin sheath before penetrating Bowman's layer and forming the sub-basal nerve plexus. This intricate network includes pain and temperature receptors, with presence of neurotrophic keratopathy having important implications for ocular surface integrity and health. These include inadequate wound healing and vulnerability to dry eye problems.[2]

In vivo confocal microscopy (IVCM) is a noninvasive tool that can be used to investigate nerve morphology and changes in the human cornea.[3] Patel and McGhee[4] used this platform to delineate the structure of the central nerve plexus and demonstrated whorl-like patterns, similar to those seen in the epithelium. The IVCM has been used in the context of characterizing changes following refractive surgery and in disease, such as keratoconus, dry eye, all forms of infective keratitis, and herpes zoster ophthalmicus.[5–8] Using in-house image analysis software, IVCM has been used to show corneal changes in HSK.[9] These include an alteration in corneal backscatter and reduction in corneal nerve density compared to healthy controls.[9–11] Hamrah et al.[9] were able to demonstrate a correlation with measurable decrease in corneal sensation and, interestingly, a decrease in nerve density in the fellow eye.

Image analysis offers the potential for quantitative evaluation of nerve damage and temporal change using semi- or fully automated platforms. Image J is an open source image-analysis platform developed by the National Institutes of Health (NIH; Bethesda, MD, USA; available in the public domain at http://rsb.info.nih.gov/ij/) and includes several line drawing tools. The segmented line drawing tool, for example, may be used to draw and quantify the length of linear structures, such as nerves. Neuron J is a semiautomated nerve-tracing plugin providing accurate nerve measurements when calibrated and can be freely downloaded from the public domain at http://www.imagescience.org/meijering/software/neuronj/.[12] Neuron J intuitively draws a line over the center of a visible nerve fiber as the nerve is traced. Several nerves can be traced without having to clear previous traces from the screen as required in Image J, potentially expediting the use of Neuron J to quantify nerves. The use of a semiautomated platform offers relative control over image analysis compared to fully automated systems. Although quantification of corneal nerve density in microbial keratitis and herpes zoster ophthalmicus has been described using both platforms, to our knowledge direct comparisons and reliability have not been assessed and for HSK.[8,13]

In this study, we sought to quantify the corneal nerve plexus density in patients with HSK, and to determine a method to assess captured images within a reasonable time frame to define its suitability as a useful clinical tool. We assessed the reliability and speed of use for Image J and Neuron J, confirming a relationship to clinically observed damage.

Methods

Patient Identification and Assessment

A total of 14 patients (16 eyes) with known HSK was identified from the corneal and external disease service at the Birmingham and Midland Eye Centre (Birmingham, UK). A service evaluation to assess Image J combined with Neuron J as a tool to quantify corneal nerve plexus density was done with approval from Sandwell and West Birmingham Hospitals NHS Trust Research and Development Department, following the tenets of the World Medical Association's Declaration of Helsinki.

Clinical examination was undertaken by one observer (GPW) and in vivo confocal microscopy by one experienced operator (PC). In the absence of an agreed and validated HSK-related opacification index, ordinal grading for opacification was determined based on a modification of the four-point grading scale used by Sotozono et al.,[14] graded from 0 to 3 (0, clear cornea with iris details clearly visualized; 1, corneal opacification involving less than 1/3 of the cornea "mild scarring"; 2, corneal opacification involving between 1/3 and 2/3 of the cornea "moderate scarring"; and 3, corneal opacification involving greater than 2/3 of the cornea "severe scarring"). Visual acuity was measured by LogMAR. Central corneal IVCM images were taken using Heidelberg HRT3 equipped with a Rostock Corneal Module (Heidelberg Engineering GMBH, Heidelberg, Germany). Two drops of oxybuprocaine 0.4% were instilled, followed by GelTears carbomer gel (Chauvin Pharmaceuticals Ltd., Surrey, UK) as a coupling agent between the ocular surface and TomoCap disposable head. Full thickness "volume" scans were performed in three locations (followed by additional "sequence" scans concentrated at the level of the nerves). For each eye, three representative images showing clearly the sub-basal nerves were selected from between 40 and 60 μm in depth from three different central corneal locations (PC).

Assessment of Corneal Nerves

For each eye, one image was duplicated and rotated at 90° or 180°, to be used in the assessment of intraobserver reliability. This gave a total of 64 images, which were sorted into a random order using the "Rand()" function in Excel for Windows (2011; Microsoft Corporation, Redmond, WA, UA) (JH) before being presented to two masked observers (SA/CJ), who had been shown how to assess nerves as outlined below, and use Image J and Neuron J. The observers were asked to count the number of nerve trunks and nerve branches. They then were asked to calculate the total nerves (number of trunks + branches). Grading of nerve tortuosity was done according to a standard subjective grading scale.[15] Finally, nerve length was measured using Image J and combined with the plugin Neuron J. Clearly visible nerves were identified and observers were asked to record the time taken to count nerves, then the time to measure nerves using each method. A separate training set of images was presented before the complete set to ensure that no learning effect could affect the final results.

Image J and Neuron J

Images were opened in Image J (available in the public domain at http://rsb.info.nih.gov/ij/) and frames calibrated to 400×400 μm. An output table was used to record data and the segmented line drawing tool used to draw all nerve trunks and branches seen as described previously.[16] Subsequently, the same image was used with the Neuron J plugin and the process repeated (Supplementary Videos S1, S2). When nerve tracings deviated the image was anchored and the drawing continued. All data were transferred to IBM SPSS 19 (IBM Corp., Armonk, NY, USA) and density calculated as nerve length in mm/mm^2.

Statistical Analysis

Agreement was quantified using intraclass correlation coefficients (ICCs). A 2-way mixed model with absolute agreement was used, and the quoted coefficients are those for average measures. The factors being compared all followed skewed distributions, and so were $\log_{10}$-transformed before analysis.

Four sets of comparisons were made. For the intraeye reliability, ICCs were calculated across the sets of three images that came from the same eye, to test whether measurements were consistent, regardless of the position on the central cornea that the image was taken. For the intraobserver reliability, the measurements for the first image for each eye and the same image after being rotated were compared to test the consistency of the observers. For interobserver reliability, the mean measurements for each of the 16 eyes were compared between the two observers to test whether the different observers gave consistent measurements. Finally, the interplatform reliability was calculated by comparing the measurements of the 48 images between Image J and Neuron J.

To further validate agreement for nerve density, the analyses above were repeated using the Bland-Altman (BA) methodology.[17] The BA plots were produced, and the mean differences within paired values assessed using paired *t*-tests. In addition to this, 95% limits of agreement (LoA) were calculated as ± 1.96 times the SD of the paired differences, to give an indication of the variability in paired measurements. The average of these limits are shown in the Tables, and the upper and lower limits of the LoA are shown in the Figures.

The overall mean nerve density across the three images and two platforms (i.e., six measurements) then was calculated for

Table 1. Summary of Average Nerve Trunks, Branches, Number of Nerves and Tortuosity; Nerve Density and Times for Both Observers to Complete Assessment in HSK

Measurement	Observer 1	Observer 2	Average
Nerve trunks	3.0 (2.0–4.0)	3.5 (2.0–5.0)	3.0 (2.0–5.0)
Nerve branches	3.0 (1.3–6.0)	4.0 (1.0–8.0)	3.0 (1.0–7.8)
Total nerves*	7.0 (3.3–10.0)	7.5 (4.3–13.0)	7.0 (4.0–11.0)
Tortuosity	1.0 (0.0–2.0)	2.0 (1.0–2.0)	1.0 (1.0–2.0)
Nerve density mm/mm^2			
Image J	6.9 (3.0–10.7)	8.5 (3.7–11.2)	7.2 (3.3–11.2)
Neuron J	6.8 (3.2–10.5)	7.9 (3.5–11.5)	7.1 (3.3–11.2)
Time to completion, s			
Image J	89.2 (35.4–138.1)	102.0 (38.5–161.0)	93.5 (35.4–140.8)
Neuron J	50.0 (18.2–71.5)	48.5 (21.5–88.8)	49.5 (21.0–80.3)

Data are reported as medians and quartiles. $P < 0.05$ was considered as significant (Wilcoxon signed rank test).
* Total nerves = total trunks + total branches.

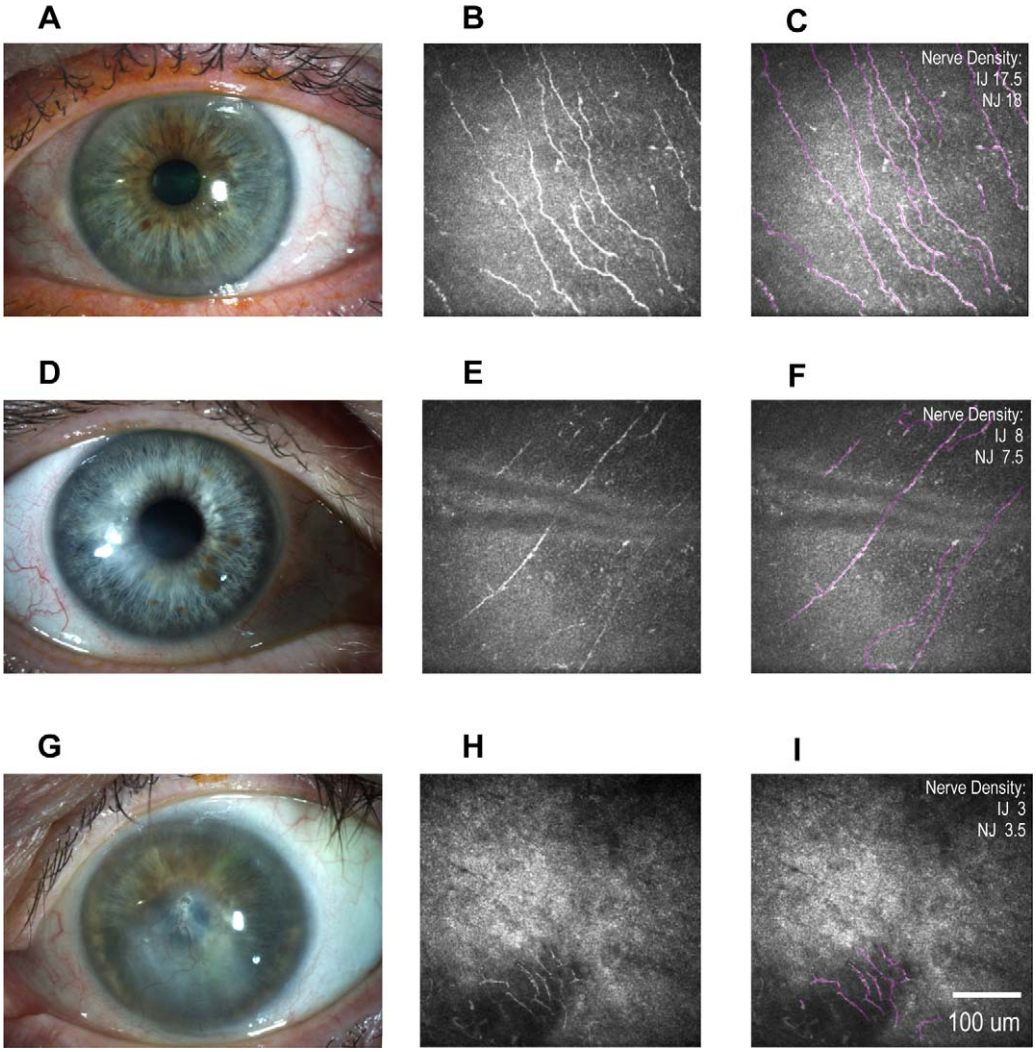

Figure 1. Representative photographs of HSK scarring with corresponding in vivo confocal images from the central cornea and Neuron J overlay of nerves. Patients with mild (<1/3 corneal opacification; [**A–C**]), moderate (1/3–2/3 corneal opacification; [**D–F**]), and severe (>2/3 corneal opacification, [**G–I**]) scarring are shown and Neuron J overlay is outlined in *purple*. The average nerve densities as calculated by Image J (*IJ*) and Neuron J (*NJ*) for both observers are shown in mm/mm^2.

Investigative Ophthalmology & Visual Science

Table 2. Intraeye and Intraobserver Agreement Between Observer 1 and 2 for Nerve Measurements in HSK

	ICC* for 3 Images of the Same Eye, Intraeye Reliability			ICC* for 2 Identical Images, Intraobserver Reliability		
Measure/Observer	**ICC***	***P* Value**	**LoA**	**ICC***	***P* Value**	**LoA**
Nerve trunks						
1	0.73 (0.37, 0.90)	0.001†	±3.68	0.85 (0.59, 0.95)	<0.001†	±2.42
2	0.80 (0.54, 0.92)	<0.001†	±3.44	0.94 (0.82, 0.98)	<0.001†	±2.05
Nerve branches						
1	0.34 (−0.53, 0.75)	0.165	±11.45	0.93 (0.80, 0.98)	<0.001†	±3.75
2	0.63 (0.13, 0.86)	0.012†	±13.28	0.96 (0.87, 0.99)	<0.001†	±6.67
Total nerves‡						
1	0.66 (0.23, 0.87)	0.006†	±11.73	0.97 (0.90, 0.99)	<0.001†	±3.65
2	0.78 (0.51, 0.92)	<0.001†	±13.36	0.98 (0.94, 0.99)	<0.001†	±6.85
Tortuosity						
1	0.41 (−0.41, 0.78)	0.115	±2.39	0.70 (0.20, 0.89)	0.009†	±1.71
2	0.60 (0.11, 0.85)	0.014†	±2.62	0.97 (0.91, 0.99)	<0.001†	±0.87
Nerve density,§ (Image J)						
1	0.83 (0.62, 0.94)	<0.001†	±8.88	0.99 (0.98, 1.00)	<0.001†	±2.17
2	0.85 (0.66, 0.94)	<0.001†	±9.82	1.00 (1.00, 1.00)	<0.001†	±1.18
Nerve density,§ (Neuron J)						
1	0.84 (0.63, 0.94)	<0.001†	±8.78	0.99 (0.96, 0.99)	<0.001†	±2.83
2	0.85 (0.65, 0.94)	<0.001†	±9.85	0.99 (0.96, 1.00)	<0.001†	±2.96

All variables were $\log_{10}$ transformed before the analysis to normalize their distributions. LoA, the average of the upper and lower limits of agreement from the BA plot.

* A2-way mixed model with absolute agreement, average measures.

† Significance, $P < 0.05$.

‡ Total nerves = total trunks + total branches.

§ Nerve density is expressed in mm/mm^2.

each eye. These values were compared across clinical factors using the Wilcoxon signed rank test and Jonckheere-Terpstra tests, as applicable. Analyses were performed using IBM SPSS 19 (IBM Corp.), and Prism version 5.0 for Macintosh (GraphPad Software, La Jolla, CA, USA) with $P < 0.05$ deemed to be indicative of statistical significance.

Results

The 14 patients in the cohort had a median age of 60 years (range, 29–83 years), and 8 (57%) were male. The median best-corrected visual acuity was 0.36 (range, 0.00–0.82) with two patients at counting fingers acuity. Opacification was graded as 0 in 2/16, mild in 4/16, moderate in 9/16, and severe in 1/16 eyes. The median disease duration was 7 (range, 1–41) years. Six patients were on long-term prophylaxis with oral acyclovir (400 mg twice daily). Three had experienced a single relapse and one had experienced two relapses in the 12 months before evaluation. One patient had epithelial disease alone and the remainder had stromal involvement.

The average numbers of nerves, branches, tortuosity, and density are outlined in Table 1. Nerve length analysis was performed by Image J and Neuron J sequentially and timed (Table 1). Representative images together with in vivo confocal and Neuron J tracings are illustrated in Figure 1.

Intraeye Reliability

Nerve density was the measurement with the best agreement across the three images from each eye, with ICCs ranging from 0.83 to 0.85 ($P < 0.001$) across the different platforms and observers (Table 2). Direct comparisons among all three images from each eye were not possible by BA; hence, the three possible pairs of images for each eye were analyzed simultaneously. This gave consistent results across the different observers and platforms, with average mean differences of −1.7 mm/mm^2 (average LoA, ±8.88) for observer 1 and −2.18 (LoA, ±9.82) for observer 2 using Image J, and −1.76 (LoA, ±8.78) for observer 1 and −2.29 (LoA, ±9.85) for observer 2 using Neuron J. This suggested that, despite nerve density having the best intraeye reliability, measurements from scans taken from different areas in the central cornea still were highly variable, with LoAs in the region of ±9.

The lowest levels of agreement for intraeye reliability were seen in the numbers of nerve branches (ICC, 0.34, 0.63 [Observer 1, Observer 2]) and tortuosity (ICCs, 0.41, 0.60).

Intraobserver Reliability

When duplicate images were presented in a random, inverted/flipped sequence, there was good intraobserver agreement for all analyses parameters (Table 2). Measurements of nerve density were the most reliable, ICCs of 0.99 or 1.00 ($P < 0.001$) for observers 1 and 2 using either Image J or Neuron J (Figs. 2A, 2B). This was confirmed by the BA plots (Figs. 2C, 2D) with mean difference measured at <–0.2 mm/mm^2 (absolute mean difference, <0.9) and average LoAs < ±3 for both observers using both platforms. This demonstrates consistency over repeated reviews of the same image by an observer.

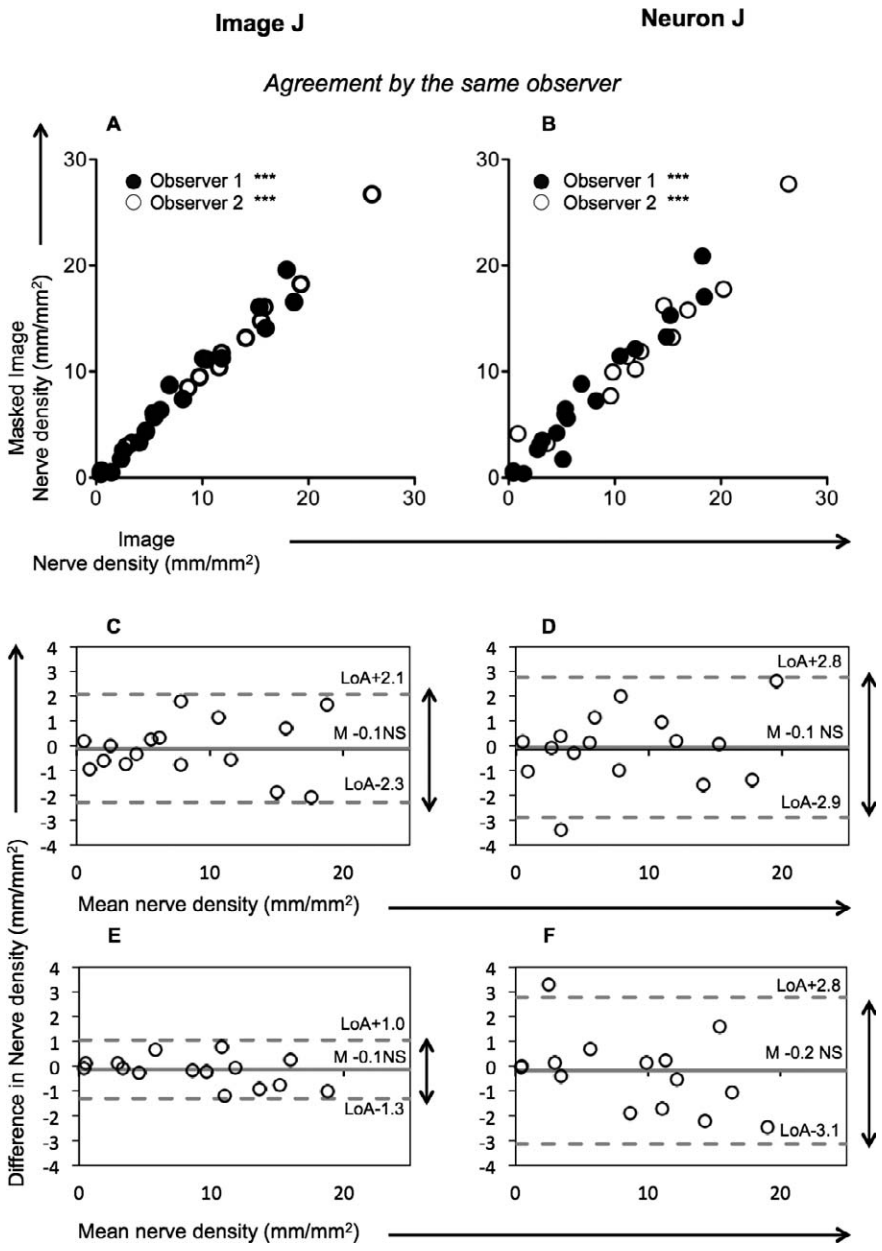

FIGURE 2. Agreement by the same observer using Image J and Neuron J for corneal nerve density in HSK. Comparison by intraclass correlation of nerve density between the same image and a masked image presented randomly in a series (intraobserver agreement) for observers 1 and 2 using Image J (**A**) and Neuron J (**B**) are expressed in mm/mm^2. The BA plots also are shown (observer 1 [**C**, **D**] and observer 2 [**E**, **F**]) to demonstrate intraobserver agreement using Image J (**C**, **E**) and Neuron J (**D**, **F**). The mean (*M*) difference is expressed together with the upper and lower 95% LoA from the mean difference (defined as ±1.96 SD [*arrow*] and termed LoA). Significance: NS, not significant; $^*P < 0.05$, $^{**}P < 0.01$, $^{***}P < 0.001$.

Interobserver Reliability

Interobserver reliability of nerve analysis also was high for all of the measures considered (Table 3). Both platforms returned ICCs of 0.96 ($P < 0.001$) for nerve density (Figs. 3A, 3B). However, the BA plots showed significant bias ($P = 0.005$ and 0.008 for Image J and Neuron J, respectively), with observer 2 consistently returning higher measurements, with an average difference of approximately 1.3 mm/mm^2. This also can be observed in Table 1, with observer 2 recording higher median numbers of nerves, trunks, and branches.

Despite the significant bias, the variability in the measurements were more reasonable, with average LoAs of ±3.35 with Image J and ±3.11 with Neuron J. This also includes two outliers which, if removed, reduce the LoAs further, to approximately ±1.6.

Interplatform Reliability

Across the 48 images, Neuron J and Image J gave very consistent results (Figs. 4A, 4B), with ICCs of 1.0 for both observers. The BA plots (Figs. 4C, 4D) found no significant bias ($P = 0.467$, 0.115 for observers 1 and 2, respectively), and relatively small average LoAs of ±1.31 for observer 1 and ±1.12 for observer 2 (average difference 0.07 and –0.13 mm/mm^2 for observers 1 and 2, respectively).

Table 3. Interobserver Agreement Between Observer 1 and 2 for Nerve Measurements in HSK

Measure	ICC* Between Observers (Interobserver Reliability)	*P* Value†	LoA
Nerve trunks	0.90 (0.62, 0.97)	<0.001	±2.07
Nerve branches	0.97 (0.91, 0.99)	<0.001	±3.80
Total nerves‡	0.97 (0.88, 0.99)	<0.001	±4.34
Tortuosity	0.81 (−0.16, 0.96)	<0.001	±0.67
Nerve density,§ Image J	0.96 (0.75, 0.99)	<0.001	±3.35
Nerve density,§ Neuron J	0.96 (0.83, 0.99)	<0.001	±3.11

All variables were $\log_{10}$ transformed before the analysis to normalize their distributions. LoA, The average of the upper and lower limits of agreement from the BA plot.

* A 2-way mixed model with absolute agreement, average measures.

† Significance at $P < 0.05$.

‡ Total nerves = total trunks + total branches.

§ Nerve density is expressed in mm/mm^2.

Timing

Images took significantly less time to assess using Neuron J than Image J, with median times of 50 seconds (quartiles, 18.2–71.5) vs. 89 seconds (35.4–138.1) for observer 1 and 49 seconds (21.5–88.8) vs. 102 seconds (38.5–161.0) for observer 2 (Wilcoxon sign ranked test, both $P < 0.001$).

Comparisons With Clinical Findings

The data were used to undertake a preliminary analysis of corneal sequelae. Diminished nerve density was associated with corneal opacification and reduction in visual acuity (Jonckheere-Terpstra test, both $P = 0.03$). There was no association with duration of disease ($P = 0.56$). However, due to low statistical power as a result of the small sample size, it is possible that this nonsignificance may be as a result of a false negative error.

Discussion

Objective monitoring of disease activity and damage in HSK also is challenging, not least because of the numerous and overlapping corneal sequelae resulting from recurrence, and the absence of agreed and validated HSK-specific activity and damage indices. Ancillary tools to clinical documentation may help the process of documentation and monitoring of disease. For instance, potentially reversible disease activity can be monitored through IVCM by measuring corneal back-scatter,

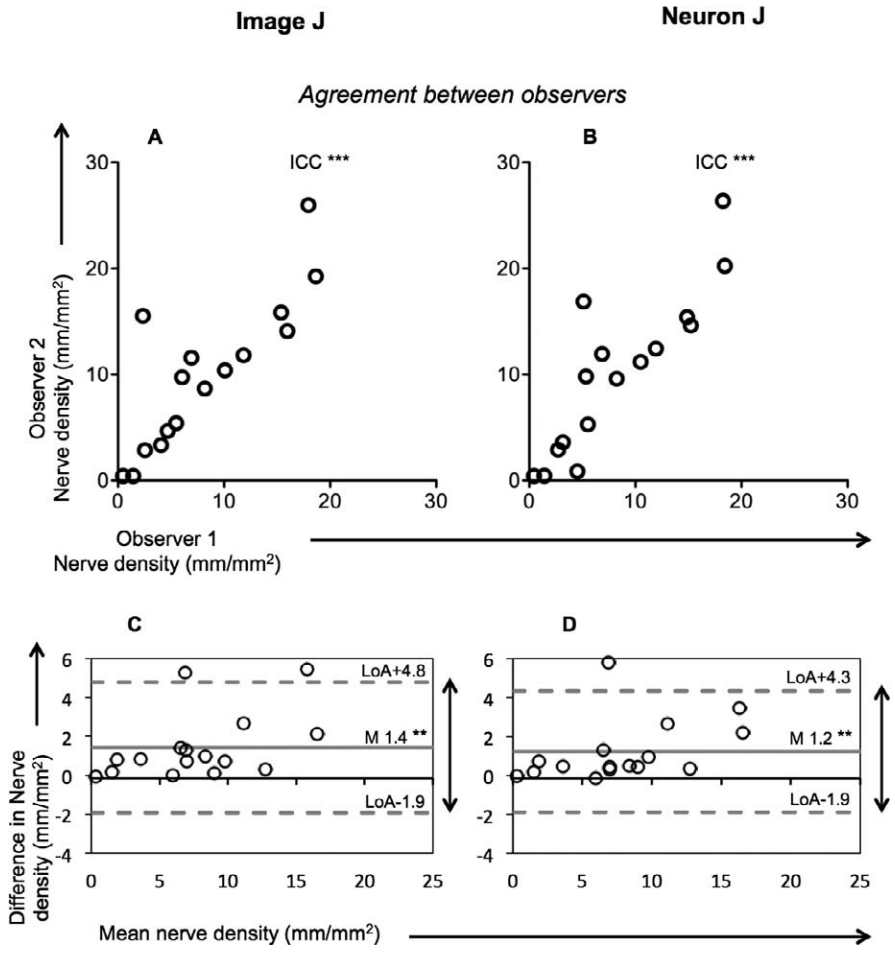

Figure 3. Agreement by different observers using Image J and Neuron J for corneal nerve density in HSK. Comparison by intraclass correlation of nerve density between observers using Image J (**A**) and Neuron J (**B**) are shown (interobserver agreement) are expressed in mm/mm^2. The BA plots are shown (**C**, **D**) to demonstrate interobserver agreement using Image J (**C**) and Neuron J (**D**). The mean (*M*) difference is expressed together with the upper and lower 95% LoA from the mean difference (defined as ±1.96 SD [*arrow*] and termed LoA). Significance: NS, not significant; $^*P < 0.05$, $^{**}P < 0.01$, $^{***}P < 0.001$.

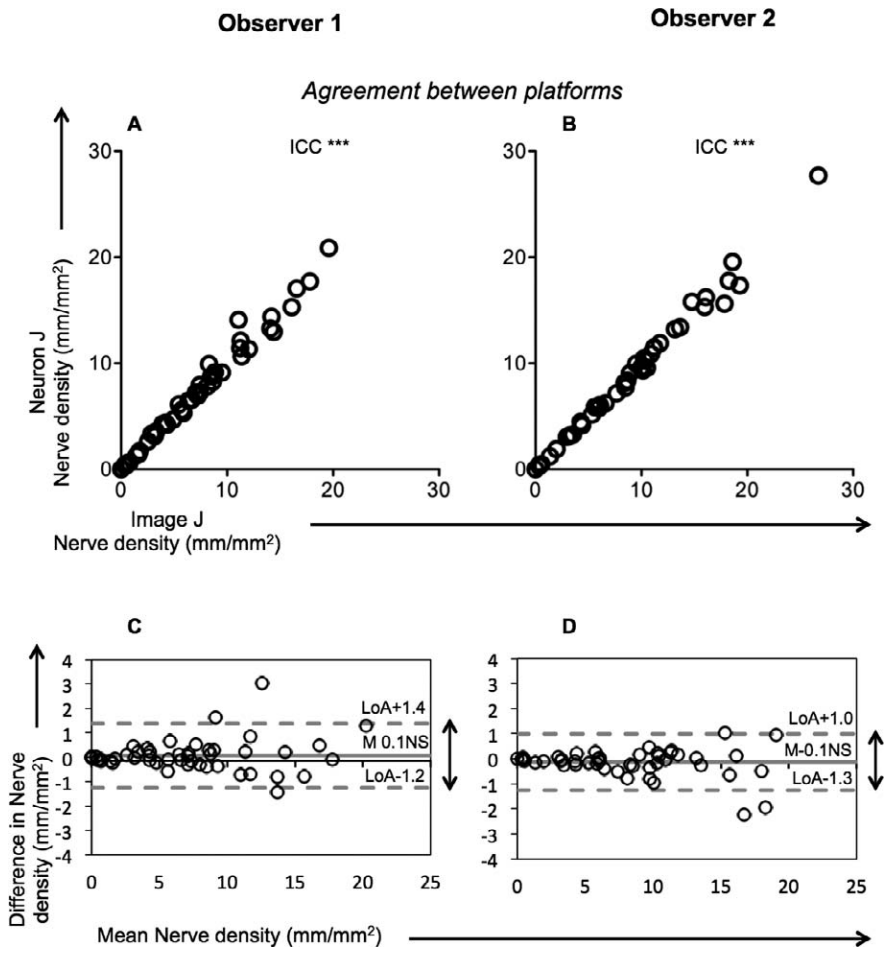

FIGURE 4. Agreement by different platforms (Image J versus Neuron J) for corneal nerve density in HSK. Comparison between Image J and Neuron J for the same image for observer 1 (**A**) and 2 (**B**). Nerve density is expressed in mm/mm^2. The BA plots are also shown (**C**, **D**) to demonstrate interplatform agreement for observer 1 (**C**) and observer 2 (**D**). The mean (*M*) difference is expressed together with the 95% LoA from the mean difference (defined as ± 1.96 SD [*arrow*]) termed LoA. Significance: NS, not significant; $^*P < 0.05$, $^{**}P < 0.01$, $^{***}P < 0.001$.

thereby discriminating disease activity in corneas with existing scarring.[10] Potentially reversible vascularization may also be quantified by fluorescein/indocyanine green angiography, allowing determination of afferent and efferent vessels, and targeted intervention.[18,19] Subjective quantification of nerve damage by IVCM includes the counting of trunks and branches or grading of tortuosity,[15] complemented by calculation of nerve density within frames or through longer mapping protocols.[5–9,11,20]

With widespread introduction of IVCM into ophthalmic departments, the potential clinical application seems apparent. Observer experience has been shown previously to influence IVCM analysis of corneal disorders, such as microbial keratitis.[7] The motivation for this service evaluation, therefore, was to determine how this platform could be used, and nerve density quantified, in a practical and reproducible fashion through image analysis software, including Image J and its semi-automated plugin Neuron J.

We found that by training two medical students, with no clinical knowledge of HSK or of the clinical data relating to central corneal IVCM images, reliable nerve quantification could be produced. We undertook different assessments of reliability, including comparisons between distinct images from the same eye, masked and randomized duplicates of the same image, and comparisons between observers. These findings are consistent with other studies where Neuron J has been quantified and where experienced observers have been used.[16,21,22] Although small but significant differences were found between our inexperienced observers (mean difference, 1.4 and 1.2 mm/mm^2) the LoAs seen were relatively low at approximately ± 3. Parissi et al.[21] demonstrated that the mean difference between observers using Neuron J to determine the sub-basal nerve density was 0.84 mm/mm^2, with a 95% LoA of $+2.4$ mm/mm^2, and Dehgani et al.[16] reported 0.62 mm/mm^2 and an ICC of 0.95.[16] Although a training set was done, greater variability might also be expected among the inexperienced observers deliberately chosen for this evaluation. It is likely, of course, in clinical practice that images will be viewed and quantified by more experienced observers with greater knowledge, and in keeping with other reports.[21,23]

Our study evaluated intraobserver variability and showed that the mean difference between repeated measurements by the same observer was extremely low, highlighting the reliability of an individual observers nerve tracings. We also considered the reliability of distinct images from the same eye. Although the ICC was relatively high, the LoA showed that recorded nerve densities varied widely depending on what point on the eye the image was taken from. This is not altogether surprising, but must be accounted for in order for the measurement of nerve density to be sufficiently consistent for prognostic/diagnostic use. A potential solution would be to

pool data from larger numbers of images scanned in the central cornea and take an average of the results.

When undertaking subjective assessments, including number of nerves/branches and tortuosity by scale, there was good agreement. The ICCs of these subjective assessments were lower, however, than the assessment by Image J and by Neuron J. Alternative tortuosity scales have been described and include the three-point scale described by Scarpa et al.,[23] which has been shown to be reliable.

The time taken to complete tasks between platforms was significantly higher with Image J than for Neuron J. The time scale of 50 seconds was comparable to those of Dehghani et al.[16] who took an average of 60 seconds to complete a frame. Time to completion is an obvious advantage of semiautomated platforms and this recent study also has shown that automated platforms, such as ACCMetrics, compare favorably with Neuron J. The intraobserver and intereye variability data, however, are not available for direct comparison with this study, and other automated platforms[24] have been found to be less reliable when compared to Neuron J.[23]

Despite the relatively small sample size, we were able to demonstrate that the extent of corneal scarring and reduction in visual acuity was inversely related to nerve density, reflecting corneal scarring. There are numerous sequelae of neurotrophic corneal damage and the ability to quantify these changes in terms of further vulnerability to relapse or secondary infections has not been explored to our knowledge. Hamrah et al.,[25] however, have demonstrated an association with decreased corneal epithelial cell density, suggesting a direct influence on corneal epithelial homeostasis, and others have recently outlined the association with dry eye problems in a murine model of HSK.[2] A reduction in corneal nerve density also has been demonstrated in dry eye problems independent of HSK, but whether there is a potentially important association with epithelial integrity, recurrence, and vulnerability to other infections has not been established.

Limitations in this study include the absence of an aesthesiometer to confirm correlation with sensation, and the fact that subjective assessment of corneal sensation was not associated with a reduction in corneal nerve plexus density (data not shown). We also were unable to demonstrate association with duration of disease, perhaps as a result of low statistical power, due to relatively small series in this evaluation exercise. Also, newer, recently validated grading systems, such as the QUT system, had not been described at the time of undertaking this study for comparison.[23]

The IVCM combined with Neuron J affords objective, user-friendly, and fast quantification of corneal nerve damage in HSK, even by relatively inexperienced observers. Improved consistency between disparate images must be explored further and in a larger longitudinal cohort. Furthermore, determining Neuron J's role in acute and chronic HSK is required to explore the potential of using this modality as an objective disease grading clinical tool. Nonetheless, it remains and attractive option because of its availability, ease of acquisition and usability.

Acknowledgments

The authors thank the Sandwell and West Birmingham NHS Trust Departments of Research and Development and Optometry for their support in facilitating this project.

Presented in part at the International Ocular Surface Society meeting, Orlando, Florida, United States, May 2014.

Supported by a Clinical Lectureship from the National Institute for Health Research, London, UK (GPW); the Barbara Mary Wilmot Trust Fund administered by the Birmingham Eye Foundation (Registered UK Charity 257549); and the Fight for Sight (UK) New Lecturers Grant (GPW). The authors alone are responsible for the content and writing of the paper.

Disclosure: **P. Cottrell**, None; **S. Ahmed**, None; **C. James**, None; **J. Hodson**, None; **P.J. McDonnell**, None; **S. Rauz**, None; **G.P. Williams**, None

References

1. Rowe AM, St Leger AJ, Jeon S, Dhaliwal DK, Knickelbein JE, Hendricks RL. Herpes keratitis. *Prog Retin Eye Res*. 2013;32:88–101.
2. Yun H, Rowe AM, Lathrop KL, Harvey SA, Hendricks RL. Reversible nerve damage and cornea pathology in murine herpes simplex stromal keratitis. *J Virol*. 2014;88:7870–7880.
3. Grupcheva CN, Wong T, Riley AF, McGhee CN. Assessing the sub-basal nerve plexus of the living healthy human cornea by in vivo confocal microscopy. *Clin Exp Ophthalmol*. 2002;30:187–190.
4. Patel DV, McGhee CN. Mapping of the normal human corneal sub-basal nerve plexus by in vivo laser scanning confocal microscopy. *Invest Ophthalmol Vis Sci*. 2005;46:4485–4488.
5. Hollingsworth JG, Bonshek RE, Efron N. Correlation of the appearance of the keratoconic cornea in vivo by confocal microscopy and in vitro by light microscopy. *Cornea*. 2005;24:397–405.
6. Benitez del Castillo JM, Wasfy MA, Fernandez C, Garcia-Sanchez J. An in vivo confocal masked study on corneal epithelium and sub-basal nerves in patients with dry eye. *Invest Ophthalmol Vis Sci*. 2004;45:3030–3035.
7. Hau SC, Dart JK, Vesaluoma M, et al. Diagnostic accuracy of microbial keratitis with in vivo scanning laser confocal microscopy. *Br J Ophthalmol*. 2010;94:982–987.
8. Hamrah P, Cruzat A, Dastjerdi MH, et al. Unilateral herpes zoster ophthalmicus results in bilateral corneal nerve alteration: an in vivo confocal microscopy study. *Ophthalmology*. 2013;120:40–47.
9. Hamrah P, Cruzat A, Dastjerdi MH, et al. Corneal sensation and subbasal nerve alterations in patients with herpes simplex keratitis: an in vivo confocal microscopy study. *Ophthalmology*. 2010;117:1930–1936.
10. Hillenaar T, van Cleynenbreugel H, Verjans GM, Wubbels RJ, Remeijer L. Monitoring the inflammatory process in herpetic stromal keratitis: the role of in vivo confocal microscopy. *Ophthalmology*. 2012;119:1102–1110.
11. Nagasato D, Araki-Sasaki K, Kojima T, Ideta R, Dogru M. Morphological changes of corneal subepithelial nerve plexus in different types of herpetic keratitis. *Jpn J Ophthalmol*. 2011;55:444–450.
12. Meijering E, Jacob M, Sarria JC, Steiner P, Hirling H, Unser M. Design and validation of a tool for neurite tracing and analysis in fluorescence microscopy images. *Cytometry A*. 2004;58:167–176.
13. Cruzat A, Witkin D, Baniasadi N, et al. Inflammation and the nervous system: the connection in the cornea in patients with infectious keratitis. *Invest Ophthalmol Vis Sci*. 2011;52:5136–5143.
14. Sotozono C, Ang LP, Koizumi N, et al. New grading system for the evaluation of chronic ocular manifestations in patients with Stevens-Johnson syndrome. *Ophthalmology*. 2007;114:1294–1302.
15. Oliveira-Soto L, Efron N. Morphology of corneal nerves using confocal microscopy. *Cornea*. 2001;20:374–384.
16. Dehghani C, Pritchard N, Edwards K, Russell AW, Malik RA, Efron N. Fully automated, semiautomated, and manual morphometric analysis of corneal subbasal nerve plexus in individuals with and without diabetes. *Cornea*. 2014;33:696–702.

17. Bland JM, Altman DG. Statistical methods for assessing agreement between two methods of clinical measurement. *Lancet*. 1986;1:307–310.
18. Anijeet DR, Zheng Y, Tey A, Hodson M, Sueke H, Kaye SB. Imaging and evaluation of corneal vascularization using fluorescein and indocyanine green angiography. *Invest Ophthalmol Vis Sci*. 2012;53:650–658.
19. Kirwan RP, Zheng Y, Tey A, Anijeet D, Sueke H, Kaye SB. Quantifying changes in corneal neovascularization using fluorescein and indocyanine green angiography. *Am J Ophthalmol*. 2012;154:850–858.
20. Zhivov A, Blum M, Guthoff R, Stachs O. Real-time mapping of the subepithelial nerve plexus by in vivo confocal laser scanning microscopy. *Br J Ophthalmol*. 2010;94:1133–1135.
21. Parissi M, Karanis G, Randjelovic S, et al. Standardized baseline human corneal subbasal nerve density for clinical investigations with laser-scanning in vivo confocal microscopy. *Invest Ophthalmol Vis Sci*. 2013;54:7091–7102.
22. Efron N, Lee G, Lim RN, et al. Development and validation of the QUT corneal nerve grading scale. *Cornea*. 2014;33:376–381.
23. Scarpa F, Zheng X, Ohashi Y, Ruggeri A. Automatic evaluation of corneal nerve tortuosity in images from in vivo confocal microscopy. *Invest Ophthalmol Vis Sci*. 2011;52:6404–6408.
24. Scarpa F, Grisan E, Ruggeri A. Automatic recognition of corneal nerve structures in images from confocal microscopy. *Invest Ophthalmol Vis Sci*. 2008;49:4801–4807.
25. Hamrah P, Sahin A, Dastjerdi MH, et al. Cellular changes of the corneal epithelium and stroma in herpes simplex keratitis: an in vivo confocal microscopy study. *Ophthalmology*. 2012;119:1791–1797.

Investigative Ophthalmology & Visual Science